PAPER

# NMR AND UPLC-QTOF/MS-BASED METABOLOMICS OF DIFFERENT DEVELOPMENTAL STAGES OF *CYNOMORIUM SONGARICUM*

**X.-Z. XUE[a,b], Q. ZHANG[a,c], X.-B. BI[d], Y. GONG[a], M.-L. WANG[a], J.-H. WANG[a] and J.-L. CUI*[a]**

[a]Institute of Applied Chemistry, Shanxi University, Taiyuan, Shanxi 030006, P.R. China
[b]Institute of Biotechnology, Shanxi University, Taiyuan, Shanxi 030006, P.R. China
[c]Modern Research Center for Traditional Chinese Medicine, Shanxi University, Taiyuan, Shanxi 030006, P.R. China
[d]Centre for Biomimetic Sensor Science (CBSS), School of Materials Science & Engineering, Nanyang Technological University, Singapore 637553, Singapore
*Corresponding author: Tel.: +86 3517016101
email: CJL717@163.com

## ABSTRACT

*Cynomorium songaricum* Rupr., a holoparasitic plant that grows in the desert and has important dietetic and medical value. However, the medicinal efficacy of *C. songaricum* collected in different seasons varies greatly, and the difference in the transformation and accumulation of its major metabolites is still unclear. In this paper, UPLC-QTOF/MS and NMR were used to study the metabolomics of *C. songaricum* in different growth stages, so as to explore the metabolic differences and regularity of *C. songaricum* in different phenological periods during one cycle. The results showed that there were thirty and sixteen compounds with significant differences based on UPLC-QTOF/MS and NMR, respectively, which were distributed in flavonoids, organic acids, sugars and amino acids. Among them, the content of secondary metabolites such as catechins and procyanidins accumulated more in the Unearthing (U), and Maturing (M) stages, while other differential compounds accumulated more in the Tubercle (T), Sprouting (S) and Atrophy (A) stages. The differential metabolic pathways of *C. songaricum* in different stages involved in flavonoids, sugar, amino acid and other pathways. This provides scientific basis for understand of metabolites accumulation, quality evaluation and use as medicinal materials for *C. songaricum*.

*Keywords*: parasitic plants, desert, comparative metabolomics, partial least squares, multivariate analysis

## 1. INTRODUCTION

*Cynomorium songaricum* Rupr. is native to China and parasitizes on the root of Nitraria sp., plant of the Zygophyllaceae family (CHEN *et al*., 2019). There are various bioactive substances of *C. songaricum*, which render *C. songaricum* abilities to enhance adrenocortical secretion, sex and bowel function (LIU *et al*., 2011). Modern pharmacological studies have shown that *C. songaricum* has the functions of promoting human metabolism, enhancing immune regulation, anti-cancer, anti-fatigue, anti-aging, anti-stress, scavenging free radicals, inhibiting the proliferation of HIV and maintaining the balance of trace elements in human body (CUI *et al*., 2013). Traditional medication practice believes that this is due to its unique active ingredients, such as flavonoids, triterpenoids, tannins, organic acids and polysaccharides and glycosides (CUI *et al*., 2018a). However, the contents and types of these bioactive components are greatly influenced by different developmental stages of *C. songaricum*, which is considered to be the main reason for the variation of its quality. Although the Chinese Pharmacopoeia (2015 ver.) recommends that the clinical materials of *C. songaricum* should be collected in spring (Committee for the Pharmacopoeia of PR China, 2015), the ethnic minorities living in the desert believe that *C. songaricum* works best if the plants were collected from the coldest winter (around November). After snowing, they often dig deep in the depths of the ground without snow and obtain high-quality *C. songaricum*. Therefore, it is generally believed that *C. songaricum* collected in other periods except winter and spring, especially at the period after flowering, has poor quality (CHANG *et al*., 2007). In fact, due to the comprehensive influence of gene timing regulation, metabolic transformation of substances and changes of external environment factors, the growth and composition of metabolites of medicinal plants should be different in each developmental period, which form the timeliness characteristics of traditional Chinese medicine (CUI *et al*., 2018b).

In the past, the quality control of *C. songaricum* depends on the contents of several main active ingredients. For example, the evaluation of *C. songaricum* in Chinese Pharmacopoeia depends on the contents of ursolic acid and proline, and in folk practice, polysaccharides, protocatechuate and catechin were also used as evaluation criterion (CUI *et al*., 2018c). However, the metabolites are mutual transformed all the time, and their accumulations vary under different spatial-temporal conditions. For example, it was reported that the contents of protocatechuate, ursolic acid, catechin and other main compounds of *C. songaricum* changed with different growth periods, which could be used as the quality evaluation and control of *C. songaricum* (CUI *et al*., 2018c). However, it should be noted that just detection of several limited ingredients cannot reflect objectively the pharmacological activity of traditional Chinese medicine, especially for *C. songaricum* which always play a role as a whole (MUHAMMAD *et al*., 2016). Because there are thousands of chemical components in *C. songaricum*, and the real quality change should be comprehensively tested for all types of metabolites and their content differences (Johnson *et al*., 2016). Therefore, in order to overcome the drawbacks such as the deficiency of mono component index, non-objective, and methodological insensitivity in traditional methods, the cutting-edge spectroscopy and chromatography-based metabolomics methods combined with multivariate statistics are highly demanded for the high-throughput analysis of metabolites of plant extracts, which can provide a comprehensive and objective evaluation of *C. songaricum* quality (ZAMPIERI *et al*., 2017).

At present, there are several platforms that have been widely used in plant metabolomics research, such as ultrahigh-performance liquid chromatography linked to quadruple time-of-flight mass spectrometry (UPLC-QTOF/MS), gas chromatography-mass spectrometer

(GC-MS), nuclear magnetic resonance (NMR), fourier transform infrared spectrometer (FTIR), capillary electrophoresis (CE) (GHATAK *et al*., 2018). However, each platform has its inherent limitations. For example, FTIR can distinguish differences in compounds, but it only focuses on the identification of chemical group without additional information such as molecular weight; UPLC-QTOF/MS and GC-MS rely solely on retention time and molecular weight to identify compounds without identifying the spectral structure of compounds; NMR is used for chemical analysis based on magnetic resonance spectroscopy but without molecular weight data (RAJU *et al*., 2017). In addition, for the same batch of plant samples, the results of metabolic difference under multivariate statistics are also generally different when the above-mentioned different metabolic platforms are used for metabolic profiling analysis (DESHMUKH *et al*., 2016). However, if two or more platforms are applied to metabolomics analysis for cross validation, the above shortcomings could be greatly reduced, and they have the advantages of mutual complementation, coordination, objectivity, comprehensiveness, accuracy, etc., which will be more of scientific value for the understanding of plant metabolic difference.
In this study, UPLC-QTOF/MS and NMR were simultaneously used to study the metabolic profile of *C. songaricum*, and to explore the differential chemical composition and metabolic pathways of *C. songaricum* in different developmental stages. We aimed at answering the questions: (i) what are the differences of the metabolome analyzed based on the two mentioned platforms? (ii) which specific metabolites are common differential products of *C. songaricum* in different developmental stages? (iii) when is the reasonable harvesting period and what is their chemical characteristic? (iv) what is the metabolic pathway of the differential metabolites in *C. songaricum*? To our knowledge, this study will systematically and objectively study the metabolites and their metabolic traits in different developmental stages of *C. songaricum* for the first time, especially clarify the composition and differences of main secondary metabolites, so as to improve the quality evaluation system of *C. songaricum* and provide scientific basis for the production and drug use of *C. songaricum*.

## 2. MATERIALS AND METHODS

### 2.1. Plant sample collection

*C. songaricum* collected from Xilin-gaole town (39° 05′ 45″ N, 105° 23′ 27″ E, ≈1133.98 m), Alashan League, Inner Mongolia of China from November of 2017 to September of 2018. The developmental stages are divided into five periods in one cycle: Tubercle (T), Sprouting (S), Unearthing (U), Maturing (M) and Atrophy (A) stages in around November (the previous year), March, May, June and September, which was described clearly in our published papers[8]. Ten samples as replicates were randomly collected from each developmental stages. The collected rhizome of *C. songaricum* was cleaned with running water, dried at 35°C, crushed and passed through the No. 4 sieve for compound extraction. They were identified by Dr Jinlong Cui, a professor at the Shanxi University (Shanxi, China). The voucher specimens (CSR20171101-20171110, CSR20180301-20180310, CSR20180501-20180510, CSR20180601-20180610 and CSR20180901-20180910) have been deposited at the biochemical laboratory of Institute of Applied Chemistry of Shanxi University.

## 2.2. Plant extraction and NMR analysis

200 mg of dry powder of *C. songaricum* was put in 25 mL triangular flask, and 10 mL of 80% methanol was added to flask followed by vortexing for 1 min and ultrasonicating (210 W, 40 kHz) for 25 min. The extraction was centrifuged at 3500 r/min for 25 min, then the supernatant was concentrated with rotary vacuum evaporator and 400 μL buffer (buffer preparation: weigh 1.232 g of $KH_2PO_4$ dissolved in $D_2O$, add 50 mg 0.05% w/v Trimethyl silyl propanoic acid (TSP), make up to 10 mL, adjust the pH to 6.0 by 1 mol/L NaOD) to dissolve the sample. After transferred to a 1.5 mL microtube and centrifuged at 13,000 r/min for 10 min, the supernatant (600 mL) was transferred into a 5 mm NMR tube for NMR analysis. Ten repeats were carried out. Analytical grade methanol was purchased from Beijing Chemical Works (Beijing, China). $D_2O$ (99.9 atom % D) and methanol-$D_4$ (D, 99.8%) were obtained from Qingdao Tenglong Weibo Technology Co., Ltd. (Qingdao, China). TSP was bought from Cambridge Isotope Laboratories Inc. (Andover, MA) and NaOD was purchased from Armar (Dottingen, Switzerland).

$^1$H-NMR was recorded at 25°C on a Bruker 600-MHz AVANCE III NMR spectrometer (600.13 MHz proton frequency). Each $^1$H-NMR spectrum consisted of 64 scans requiring 5 min acquisition time with the following parameters: relaxation delay = 1.0 s, pulse width = 14.0 μs, and spectral width = 12345.7 Hz. A pre-saturation sequence was used to suppress the residual $H_2O$ signal with low power selective irradiation at the $H_2O$ frequency during the recycle delay. $CD_3OD$ was used for internal lock purposes. The resulting spectra were manually phased and baseline-corrected, and calibrated to TSP at 0.00 ppm for water fractions (ZHI *et al*., 2012).

## 2.3. Plant extraction and UPLC-QTOF/MS analysis

Two grams of dried powder of *C. songaricum* was weighed into a 50 mL flask, followed by the addition of 20 mL of extraction solution (methanol:water = 4:1) to each sample and extraction with an ultrasonic method (210 w, 40 kHz) for 30 min. The extracted suspension was centrifuged at 12000 rpm at 4 °C for 6 min twice, and their resulting supernatants were combined and dried with rotary vacuum evaporator, and then reconstituted to 10 mL with acetonitrile:water = 1:9. Ten random samples as repeats were performed in each development stage. Quality control (QC) samples were made by equal proportional mixing of all samples. All samples, including the QC samples, were passed through as 0.22 μm syringe filter before MS analysis**.** Methanol (HPLC grade, purity≥99.9%) and acetonitrile (LC/MS grade, purity ≥ 99.9%) were purchased from Thermo Fisher Scientific Co., (Shanghai Pudong New District, Shanghai, China), the water was purified by Ultrapure Water Systems ($H_2O$pro-VF-T-TOC, Sartorius, Germany).

The metabolites were analyzed and detected using Agilent 6545 UPLC-QTOF/MS (Agilent Technologies, USA) with positive ion mode (+ESI). After the optimization of experimental conditions, a method was established for the non-target metabolomics profiling of secondary metabolites in *C. songaricum*. Samples were analyzed in random order, and one injection of QC sample was inserted for each set of five samples as quality control standards during data acquisition. The samples were separated by SB C18 column (1.8 μm particle size, 4.6 x 50 mm; Agilent Technologies, USA), and maintained at 40 °C. The mobile phase solvent A consisted of 0.1% formic acid in water, and solvent B was pure acetonitrile. The flow rate used for separation was 0.25 mL/min, with an injection volume of 10 μL, and the gradient program used constituted 0-5 min, 10%-20% B; 5-7 min, 20%-50% B; 7-9 min, 50%-55% B; 9-11 min, 55%-60% B; 11-13 min, 60%-65% B; 13-15 min,

65%B. Ion spray voltage was 4.4 kV; nebulizer voltage was 1.5 kV; dry gas rate and temperature were 5 L/min and 300°C; sheet gas flow rate and temperature were 12 L/min and 270°C; collision energy was 140 V. The spectra were collected in full scan mode from 80 to 1200 m/z.

### 2.4. Data statistics and analysis

The $^1$H-NMR spectra were processed using MestReNova (version 6.1.0-6224, Mestrelab Research, Santiago de Compostella, Spain). After TSP correction, phase adjustment and baseline adjustment for all $^1$H-NMR spectra, spectral intensities were scaled to total intensity and reduced to integrated regions of equal width (0.01 ppm) corresponding to the region of δ 0.60-10.00. The regions of δ 4.80-4.95 and δ 3.32-3.34 were excluded from the analysis because of the residual signals of water and methanol, respectively. The pre-processing of raw data from UPLC-QTOF/MS performed with Masshunter Quality analysis software (Agilent Technologies, USA) to de-convolute and align the spectral peaks, then peaks normalization and retention time correction were done using XCMS online platform (https://xcmsonline.scripps.edu/).
The pre-processed data were separately exported to SIMCA-P 14.1 software (Umetrics UK Ltd, Windsor, UK) for multivariate statistical analysis to elucidate the dynamic accumulation changes of the metabolites of *C. songaricum* at different developmental stages. Principal component analysis (PCA) with unit variance scaling and orthogonal partial least squares-discriminant analysis (OPLS-DA) with Pareto scaling method were used to find class-separating differences, and cross-validation (CV) was used to determine the correctness and prevention over-fitting of the model.
According to the variable importance of projection (VIP>1) of S-plot analysis combining with a t-test (P-value<0.05), the significant differential metabolites were selected. For NMR-metabolomics studies, NMR data from the references (ZHANG *et al*., 2016; JIN *et al*., 2012; MA *et al*., 1999; JIANG *et al*., 2001; ZHANG *et al*., 2007a; ZHANG, 2007; ZHANG *et al*., 2007b; ZHANG *et al*., 1996; MA *et al*., 1993; MA *et al*., 2002; XU *et al*., 1996; WANG *et al*., 2011; HUANG, 1997; ZHANG *et al*., 1990; MENG and MA, 2013) and standard sample from the Human Metabolome Database (HMDB, www.hmdb.ca/) were used for metabolites identification of NMR spectra. For UPLC-QTOF/MS-metabolomics studies, the Pesticides Personal Compound Database and Library (PCDL), HMDB, the Massbank Database (www.massbank.jp/) and the Metlin metabolite database (https://metlin.scripps.edu/) were used for identification of differential metabolites of *C. songaricum*.
The relative contents of differential metabolites in *C. songaricum* (Ten replicates were set in each developmental stage) were analyzed using Origin software (OriginPro 2018C, OriginLab, USA). Finally, in order to further explore the metabolic mechanism of different metabolites of *C. songaricum* at different developmental stages, the metabolic pathways involved by differential metabolites were analyzed through KEGG database (www.kegg.jp/) and KEGG Compound Database (www.genome.jp/kegg/compound/).

## 3. RESULTS

### 3.1. Differential marker metabolites in *C. songaricum* based on NMR

A total of 25 metabolites of *C. songaricum* based on NMR were identified, including amino acids, such as cysteine, tyrosine, glutamate, aspartate; sugars such as sucrose, maltose and lactulose; secondary metabolites mainly include flavonoids, such as catechin, epicatechin, epicatechin-3-*O*-gallate, rutin; organic acids including malate, ursolic acid, oleanolic acid and masilinic acid. The chemical shifts and coupling constants of identified metabolites were exhibited in Table 1.

Based on a large number of fingerprint information obtained by NMR, the data were analyzed by means of multivariate statistical methods to accurately reveal the dynamic changes of metabolites in each stage of *C. songaricum*. In order to find potential biomarkers, PCA of *C. songaricum* at each development stage was carried out (Fig. 1), and the results showed distinct distribution of samples based on chemical composition from different developmental stages. It can be seen from Figure 1A**,** the sample from 'T', 'M', and 'A' stages of *C. songaricum* are located at the positive half of the PC2, while the 'S' and 'U' samples are located on the negative half of the PC2. This indicates that the metabolites of the *C. songaricum* in different developmental stages gradually change with the development of *C. songaricum*, which showed that the similar distance became further and further followed by 'T', 'S', 'U' successively, but it return from 'M', and 'A' is the closest to 'T' finally, which form a cycle like the annual development cycle of *C. songaricum* from November (the previous year), March, May, June to September which is the closest to November. The loadings plot (Fig. 1C) was used to find the metabolites that are responsible for the separation between *C. songaricum* at different development stages.

**Table 1.** Twenty-five identified metabolites including sixteen significant differential metabolites based on NMR from *C. songaricum* at different developmental stages.

| No. | Metabolites | Assignment | $\delta^1$H (ppm) | Multiplicity (*J* in Hz) |
|---|---|---|---|---|
| 1 | Cysteine* | 3-H | 3.03 | dd (11.1, 6.8) |
| | | 2-H | 3.98 | dd (5.6, 4.2) |
| 2 | Tyrosine* | 3-H | 6.85 | d (8.5) |
| | | 2-H | 7.18 | d (8.6) |
| 3 | Glutamate* | $\beta$-$CH_2$ | 1.99 | m |
| | | $\beta$-$CH_2$ | 2.08 | m |
| | | $\gamma$-$CH_2$ | 2.34 | m |
| | | $\alpha$-CH | 3.75 | dd (9.7, 19.2) |
| 4 | Aspartate | $\beta$-CH | 2.84 | dd (8.0, 17.0) |
| | | $\beta'$-CH | 2.96 | dd (4.0, 17.0) |
| | | $\alpha$-CH | 3.96 | dd (7.9, 4.0) |
| 5 | Threonine | $\gamma$-$CH_3$ | 1.35 | d (6.9) |
| | | $\alpha$-CH | 3.57 | d (5.3) |
| | | $\beta$-CH | 4.27 | m |
| 6 | Proline | $\gamma'$-$CH_3$ | 1.01 | d (7.0) |
| | | $\gamma$-$CH_3$ | 1.06 | d (7.0) |
| | | $\alpha$-CH | 3.61 | d (4.0) |

| | | | | |
|---|---|---|---|---|
| 7 | Alanine* | $\beta$-$CH_3$ | 1.49 | d (7.2) |
| | | $\alpha$-CH | 3.81 | q (7.2) |
| 8 | $\alpha$-Glucose | $C_1H$ | 5.20 | d( 3.8) |
| 9 | $\beta$-Glucose | $C_1H$ | 4.60 | d (7.9) |
| 10 | Sucrose* | Fru-$C_1H$ | 4.19 | d (8.7) |
| | | Glc-$C_1H$ | 5.42 | d (3.8) |
| 11 | Maltose* | 12-H | 3.45 | t (9.5) |
| | | 4-H | 5.27 | d (3.9) |
| 12 | Lactulose | 27-H | 4.12 | dd (7.2, 3.0) |
| | | 4-H | 4.24 | t (4.0) |
| | | 11-H | 4.44 | d (7.8) |
| | | 34-H | 4.52 | d (7.8) |
| 13 | Catechin* | 4a-H | 2.54 | dd (16.2, 8.1) |
| | | 4b-H | 2.82 | dd (15.9, 5.8) |
| | | 6-H | 5.96 | d (2.1) |
| | | 2′-H | 6.90 | d (1.9) |
| 14 | Epicatechin | 4-H | 2.91 | m |
| | | 6-H | 6.05 | d (2.0) |
| | | 5′-H | 7.03 | d (1.9) |
| 15 | Protocatechuate* | 5-H | 6.88 | d (8.1) |
| | | 6-H | 7.39 | dd (2.1, 8.2) |
| | | 2-H | 7.43 | d (2.0) |
| 16 | Vanillate* | 2′-H | 3.89 | s |
| | | 5-H | 6.88 | d (8.1) |
| | | 6-H | 7.39 | dd (2.1, 8.2) |
| | | 2-H | 7.43 | d (2.0) |
| 17 | Malate* | 3a-H | 2.46 | dd (5.3, 14.3) |
| | | 3b-H | 2.71 | dd (3.4, 15.6) |
| | | 2-H | 4.30 | dd (3.4, 9.1) |
| 18 | Masilinic acid* | 3-H | 3.31 | m |
| | | 2-H | 3.43 | m |
| | | 12-H | 5.16 | s |
| 19 | Ursolic acid* | 29-H | 0.91 | d (6.8) |
| | | 23-H | 0.98 | s |
| | | 18-H | 2.24 | d (14.3 ) |
| | | 3-H | 3.22 | dd (6.0, 10.9) |
| | | 12-H | 5.16 | t (5.5) |
| 20 | Oleanolic acid* | 27-H | 0.88 | t (12.6) |
| | | 17-H | 1.22 | d (6.5) |
| | | 22-H | 1.85 | d (2.5) |
| 21 | Rutin* | 1′′′-H | 4.44 | d (7.8) |
| | | 6-H | 6.19 | d (2.9) |
| | | 8-H | 6.30 | d (1.7) |
| | | 5′-H | 6.85 | d (8.5) |
| 22 | Ursane-12-ene-28-acid-3$\beta$-malonate monoester | 3$\beta$-H | 4.56 | dd (3.6, 10.8) |

| | | | | |
|---|---|---|---|---|
| | | 10-H | 1.94 | s |
| 23 | 3,4-DihydroxyPhenylacetate | 7-H | 2.54 | t (8.0) |
| | | 2-H | 6.59 | d (2.2) |
| | | 5-H | 1.29 | d (6.2) |
| | | 3-H | 3.45 | t (9.5) |
| 24 | Vanillin* | 4-H | 4.10 | m |
| | | 2-H | 4.19 | d (8.7) |
| | | 4b-H | 2.82 | dd (15.9, 5.8) |
| | | 3-H | 5.51 | d (2.6 ) |
| | | 6-H | 5.98 | d (2.3) |
| | | 5′-H | 6.77 | d (8.2) |
| 25 | Epicatechin-3-*O*-gallate* | 6′-H | 6.80 | dd (2.0, 8.2) |
| | | 2′-H | 6.95 | d (1.9) |
| | | 2″-H, 6″-H | 6.99 | s |

*Sixteen metabolites with significant difference.

Cross-Validation (Fig. 1E) shows that the model has a $R^2Y$ value of 0.98 and a $Q^2Y$ value of 0.90, indicating that the model is valid to use for significant differential metabolites selection. A total of 16 differential metabolites were selected as potential biomarker (Table 1) through the S-plot of OPLS-DA (Fig. 1G).

### 3.2. Relative content fluctuation of differential metabolites based on NMR

The relative contents of 16 differential compounds were determined by NMR with TSP as internal standards. Comparing to the 'T', 'S', and 'A' stages, the contents of main differential markers were more higher from 'U' and 'M' stages, such as flavonoids, organic acids and amino acids, such as catechins, epicatechin-3-*O*-gallate, protocatechuate, malate, ursolic acid, oleanolic acid, masilinic acid, glutamate and tyrosine. Among them, their relative contents in 'M' stage are higher than those in the 'U' stage. However, the differential primary metabolites such as maltose, sucrose, and alanine have the higher contents in the 'T' and 'A' stages of *C. songaricum*, and were lower in other stages. In addition, the content of vanillate and vanillin are contrary in all stages (Table 2).

### 3.3. Selection and identification of differential metabolites based on UPLC-QTOF/MS

The differential metabolites were selected with multivariate analysis from UPLC-QTOF/MS data obtained from five developmental stages of *C. songaricum*. The data matrix was 50 × 3374 after the data normalized, and the spectra were subjected to PCA analysis. It can be seen from the constructed PCA score plot (Figure 1B) that the QC samples are concentrated at one point, and the samples from the same developmental stage are relatively concentrated together. The distribution areas are obviously distinguished but also there is overlap from 'T', 'S', 'U', 'M' to 'A', and they gradually change and form a succession cycle. The supervised statistical method, OPLS-DA, was used to analyze the differential metabolites between samples from different developmental stages.

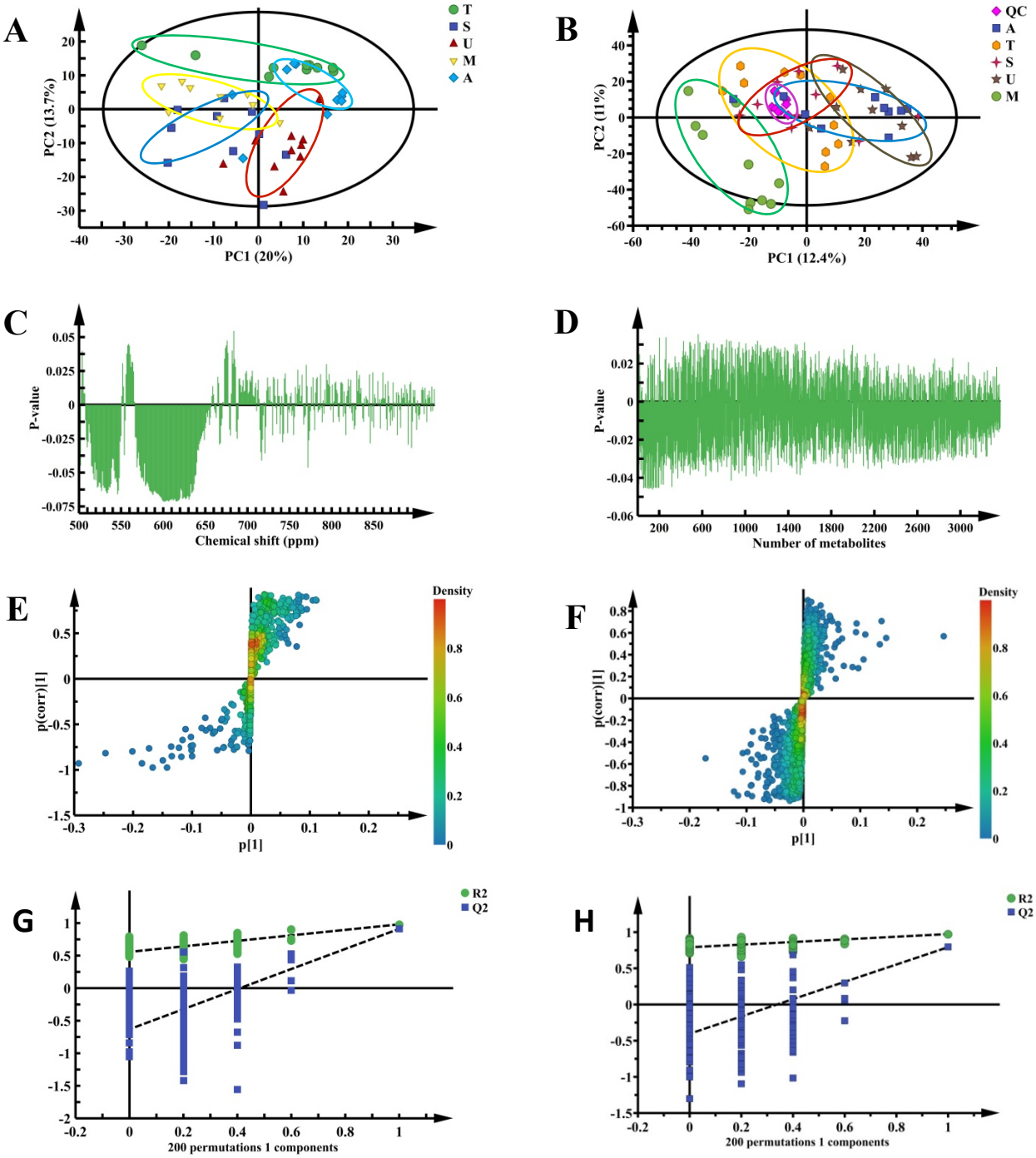


**Figure 1.** Metabolic analyses of *Cynomorium songaricum* at different developmental stages. (A, B) and (C, D) represent score and loading plot of PCA; (E, F) and (G, H) represent cross validation (CV) of the OPLS-DA model and S-plot, respectively. A, C, E and G for NMR, B, D, F and H for UPLC-QTOF/MS. 'T', 'S', 'U', 'M' and 'A' represent Tubercle, Sprouting, Unearthing, Maturing and Atrophy. CV of the PLS-DA model verifies the high predictability ($Q^2Y > 0.80$) of OPLS-DA at 'T' and 'S' stage for UPLC-QTOF/MS; ($Q^2Y > 0.91$) of OPLS-DA at 'T' and 'U' stage for NMR. The highly significant differential metabolites are included in the ellipse from the S-plot area.

It can be seen from Fig. 1F that the $R^2$ and $Q^2$ values ($R^2Y = 0.98$, $Q^2Y = 0.80$) generated by any random arrangement at the left end of the OPLS-DA permutation test (n = 200) were lower than the original value at the right end, indicating the prediction ability of real model is greater than that of any randomly arranged Y variable, which proves that the model has great predictability and goodness of fit. The score loading plot (Fig. 1D) indicated that there were at least 3365 significant difference metabolites for each development stages. Analysis by S-Plot (Fig. 1H), differential metabolites between different developmental stages of *C. songaricum* were determined by standard of VIP > 1 and *P*-value < 0.05. A total of 30 differential metabolites were selected as potential biomarker.

Combining with the m/z, retention time and MS/MS fragment of the mass spectrum in the HMDB and Massbank Database, 30 differential metabolites of *C. songaricum* were identified, including flavonoids (flavonoids and their glycosides are the main chemical constituents of *C. songaricum*), organic acids, esters, polysaccharides and other components. The metabolite M577T8 with m/z 577.1327 and its MS/MS fragmentation information (m/z 109.0290 for $C_6H_5O_2$; m/z 111.0446 for $C_6H_7O_2$; m/z 121.0290 for $C_7H_5O_2$; m/z 123.0446 for $C_7H_7O_2$; m/z 137.0239 for $C_7H_5O_3$; m/z 139.0395 for $C_7H_7O_3$; m/z 253.0501 for $C_{15}H_9O_4$; m/z 271.0606 for $C_{15}H_{11}O_5$; m/z 273.0763 for $C_{15}H_{13}O_5$; m/z 393.0610 for $C_{21}H_{13}O_8$; m/z 395.0767 for $C_{21}H_{15}O_8$; m/z 407.0767 for $C_{22}H_{15}O_8$; m/z 409.0923 for $C_{22}H_{17}O_8$; m/z 419.0403 for $C_{22}H_{11}O_9$; m/z 425.0873 for $C_{22}H_{17}O_9$ and m/z 577.1346 for $C_{30}H_{24}O_{12}$) (Fig. 2) identified as proanthocyanidin A1. Similarly, other compounds have been identified and the results are shown in Table 3.

### 3.4. The relative variation of metabolites based on UPLC-QTOF/MS

The contents of maltol, N-nitrosothiazolidine-4-carboxylic acid, phenylglyoxal, norartocarpanone, urolithin C, proanthocyanidin A1, procyanidin C1, 1D-myo-inositol 3,4-bisphosphate, HMBA, 2-methylfuran, 3,4-dihydroxyphenacyl caffeate, 3,4-dihydroxybenzaldehyde, DDDB, D-galactose, dimethyl trisulfide, 4-hydroxybenzaldehyde, 3-oxo-valproic acid CoA, 4-*O*-methylgallic acid, BR-xanthone B, aflatoxin G, kaempferol 7-(6''-galloylglucoside), epicatechin 5-*O*-*β*-D-glucopyranoside-3-benzoate is higher in the 'M' stage of *C. songaricum*, lower in the 'S' and 'U' stages, similar in the 'T' and 'A' stages. 5-ethynyl-5'-(1-propynyl)-2,2'-bithiophene was higher in the 'S' and 'U' stages of *C. songaricum*, and lower in the 'M' stage. Meanwhile, the contents of lactulose, cochliophilin A, DPCM, DPOT and 4,5-trihydroxyoxane-2-carboxylic acid are higher in the 'T' and 'A' stages than that in other stages. However, the contents of rotenone are highest in the 'T' stage, low in other stages (Table 4).

### 3.5. Comparative analysis of differential metabolic pathways based on NMR and UPLC-QTOF/MS metabolomics studies

In order to explore the metabolic differences of *C. songaricum* at different development stages, to reveal the metabolic mechanisms involved among them, metabolic pathways involved 16 and 30 differential metabolites based on NMR (Table 1) and UPLC-QTOF/MS (Table 3) were constructed with bio-information methods. It can be seen from Figs. 3 and 4, seventeen and thirty differential metabolites in NMR and UPLC-QTOF/MS involved in tricarboxylic acid cycle, shikimic acid pathway and other metabolic pathways, respectively.

**Table 2.** Changes in the accumulation of 16 differential metabolities in C. songaricum across the developmental stages of tubercle (T), sprouting (S), unearthing (U), maturing (M), and atrophy (A) developmental stage using Nuclear Magnetic Resonance (NMR) analysis. Ten samples as replicates were randomly detected from each developmental stages.

| Name | mean±SD (n = 10) | | | | |
|---|---|---|---|---|---|
| | T | S | U | M | A |
| Cysteine | 0.0035±0.0039** | 0.0542±0.0232** | 0.0735±0.0303** | 0.0135±0.0055 | 0.0206±0.0243 |
| Tyrosine | 0.0765±0.0448** | 0.1239±0.0394 | 0.0745±0.0290** | 0.1438±0.0355 | 0.0520±0.0309** |
| Glutamate | 0.2846±0.0714** | 0.4699±0.1570 | 0.3908±0.1924* | 0.6317±0.1914 | 0.5656±0.2243 |
| Alanine | 5.7626±1.8119** | 2.1460±0.9384 | 2.8296±1.0804 | 2.6147±0.8801 | 4.8527±2.1000** |
| Sucrose | 2.4065±0.4842** | 0.6419±0.4551 | 0.8578±0.3754** | 0.9822±0.4883 | 1.5574±1.0870** |
| Maltose | 1.3424±0.5816** | 0.3284±0.1618** | 0.6355±0.2986 | 0.5638±0.2933 | 1.0325±0.5912** |
| Catechin | 0.0309±0.0114** | 0.0743±0.0227* | 0.1152±0.0707 | 0.1617±0.1158 | 0.0344±0.0098** |
| Protocatechuate | 0.1341±0.0902** | 0.1886±0.0790 | 0.0951±0.0428** | 0.2456±0.0718 | 0.0818±0.0446** |
| Vanillate | 0.3579±0.0949** | 0.7761±0.2635 | 0.7822±0.2045* | 0.5851±0.1227 | 0.5174±0.2616 |
| Malate | 0.2280±0.2030** | 0.4925±0.3781 | 0.1806±0.2586** | 0.6693±0.3779 | 0.1911±0.1366** |
| Masilinic acid | 0.5366±0.3384* | 1.0722±0.4503 | 0.5505±0.3333* | 0.9427±0.3147 | 0.4148±0.1536** |
| Ursolic acid | 0.0635±0.0128** | 0.3161±0.1440 | 0.3475±0.2303 | 0.2785±0.0838 | 0.1493±0.0676** |
| Oleanolic acid | 0.0538±0.0103** | 0.1442±0.0540* | 0.2667±0.0815 | 0.2192±0.0627 | 0.1464±0.0727* |
| Rutin | 0.5695±0.4622 | 1.0686±0.4321* | 0.6821±0.4622 | 0.6294±0.6785 | 0.4572±0.3862 |
| Vanillin | 1.2766±0.4563** | 0.7753±0.3315 | 0.5978±0.2784 | 0.6088±0.4245 | 0.9992±0.6224 |
| Epicatechin-3-*O*-gallate | 0.0681±0.0436** | 0.1048±0.0403 | 0.0534±0.0283** | 0.1425±0.0552 | 0.0421±0.0267** |

$P<0.05$ and $^{**}P<0.01$ represent significant and extremely significant (*t*-test in 'T', 'S', 'U' and 'A' stages compared with 'M' stage) in curve graph of relative content of differential metabolites from different developmental stages. SD: standard deviation values.

**Table 3.** Identification of 30 differential metabolites based on UPLC-MS/MS from *C. songaricum* at different developmental stages.

| No. | Formula | Identification | RT | m/z | Major fragment ion (m/z) | VIP |
|---|---|---|---|---|---|---|
| 1 | $C_7H_6O_2$ | 4-Hydroxybenzaldehyde | 3.73 | 123.0440 | 81.0335, 91.0539, 93.0334 | 1.93 |
| 2 | $C_6H_6O_3$ | Maltol | 6.71 | 127.0390 | 95.0497, 109.0282 | 3.07 |
| 3 | $C_8H_6O_2$ | Phenylglyoxal | 3.75 | 135.0440 | 109.0282, 107.0488, 91.0539 | 2.35 |
| 4 | $C_7H_6O_3$ | 3,4-Dihydroxybenzaldehyde | 7.45 | 139.0388 | 109.0284, 121.0283, 81.0335, 107.0487, 123.0440, 111.0074, 91.0539 | 3.75 |
| 5 | $C_5H_{10}O_3S$ | HMBA[a] | 9.20 | 151.0388 | 117.0330, 115.0531, 133.0608, 135.0430, 103.0537, 85.0277 | 4.39 |
| 6 | $C_5H_6O$ | 2-Methylfuran | 2.58 | 158.9638 | 83.0486 | 1.68 |
| 7 | $C_2H_6S_3$ | Dimethyl trisulfide | 2.11 | 164.9208 | 126.9738, 80.0493 | 3.16 |
| 8 | $C_8H_8O_5$ | 4-*O*-Methylgallic acid | 2.52 | 185.0416 | 123.0438, 97.0280 | 4.35 |
| 9 | $C_{13}H_8S_2$ | 5-Ethynyl-5'-(1-propynyl)-2,2'-bithiophene | 2.54 | 192.9981 | 229.0489, 121.0281, 109.0025, 147.0436 | 3.62 |
| 10 | $C_4H_6N_2O_3S$ | N-Nitrosothiazolidine-4-carboxylic acid | 2.55 | 200.9741 | 163.0376, 111.0429, 117.0686, 114.0902, 145.0632, 111.0066, 129.0682 | 3.18 |
| 11 | $C_6H_{12}O_6$ | D-Galactose | 2.52 | 203.0524 | 163.0477, 181.9620, 133.0526 | 6.56 |
| 12 | $C_{13}H_8O_5$ | Urolithin C | 7.46 | 245.0441 | 203.0322, 201.0534, 191.0325, 177.0530, 173.0585, 161.0586, 147.0430, 145.0640, 119.0482 | 3.75 |
| 13 | $C_{14}H_{10}O_6$ | BR-Xanthone B | 8.45 | 275.0544 | 203.0525, 245.0444 | 1.62 |
| 14 | $C_{15}H_{12}O_6$ | Norartocarpanone | 8.72 | 289.0701 | 271.0598, 259.0598, 245.0442, 179.0337, 163.0390, 153.0184, 135.0440, 111.0441 | 1.09 |
| 15 | $C_{15}H_{14}O_6$ | DDDB[b] | 5.71 | 291.0858 | 139.0382, 127.0387, 163.0383, 111.0433, 153.0173 | 1.43 |
| 16 | $C_{23}H_{22}O_6$ | Rotenone | 3.46 | 365.0654 | 203.0700, 203.0474, 111.0433 | 6.64 |
| 17 | $C_{12}H_{22}O_{11}$ | Lactulose | 3.47 | 365.1047 | 181.0494, 147.0439, 119.0492, 105.0700, 93.0336 | 11.09 |
| 18 | $C_{16}H_{10}O_5$ | Cochliophilin A | 3.06 | 366.1084 | 181.0494, 151.0391, 139.0387 | 9.21 |
| 19 | $C_6H_{14}O_{12}P_2$ | 1D-Myo-inositol 3,4-bisphosphate | 2.52 | 378.9592 | 341.0056, 119.0480, 163.0741 | 1.46 |

| | | | | | | |
|---|---|---|---|---|---|---|
| 20 | $C_{15}H_{18}O_{10}$ | DPOT[c] | 3.03 | 381.0787 | 123.0443, 177.0242 | 3.74 |
| 21 | $C_{17}H_{12}O_7$ | Aflatoxin G | 6.72 | 407.0756 | 329.0633, 163.0379, 109.0644 | 1.36 |
| 22 | $C_{17}H_{14}O_7$ | 3,4-Dihydroxyphenacyl caffeate | 6.60 | 409.0910 | 151.0385, 135.0436, 139.0384, 147.0435, 163.0385, 259.0589 | 1.50 |
| 23 | $C_{27}H_{26}O_{11}$ | DPCM[d] | 2.53 | 527.1575 | 123.0441, 527.1574 | 5.41 |
| 24 | $C_{30}H_{24}O_{12}$ | Proanthocyanidin A1 | 8.44 | 577.1327 | 109.0283, 577.1328, 139.0390, 137.0235, 121.0281 | 1.60 |
| 25 | $C_{28}H_{28}O_{12}$ | Epicatechin 5-*O*-*β*-D-glucopyranoside-3-benzoate | 8.72 | 579.1483 | 109.0284, 111.0439, 123.0442, 123.0391, 289.0707 | 1.49 |
| 26 | $C_{28}H_{24}O_{15}$ | Kaempferol 7-(6''-galloylglucoside) | 3.46 | 601.1306 | 287.0535, 95.0484, 245.0426, 601.1282 | 1.26 |
| 27 | $C_{45}H_{38}O_{18}$ | Procyanidin C1 | 3.46 | 889.1938 | 139.0379, 151.0381 | 1.83 |
| 28 | $C_{29}H_{48}N_7O_{18}P_3S$ | 3-Oxo-valproic acid CoA | 3.46 | 890.1967 | 107.0482, 287.1435 | 1.08 |
| 29 | # | Compound 1 | 2.04 | 90.9765 | 122.9245,108.9619,112.8957, 84.9597,80.9670 | 3.75 |
| 30 | # | Compound 2 | 1.97 | 108.9619 | 84.9598, 182.9624, 198.9398, 110.9600, 80.9670 | 2.40 |

RT = Retention time; VIP = variable importance in projection.

[a]HMBA: (±)-2-Hydroxy-4-(methylthio)butanoic acid.

[b]DDDB: 3-(3,4-dihydroxyphenyl)-3,4-dihydro-2H-1-benzopyran-4,6,7-triol.

[c]DPOT: 6-{[3-(3,4-dihydroxyphenyl)propanoyl]oxy}-3,4,5-trihydroxyoxane-2-carboxylic acid.

[d]DPCM: 6-(2-{8,8-dimethyl-2-oxo-2H,8H-pyrano[2,3-f]chromen-3-yl}-5-methoxyphenoxy)- 3,4,5-tri-hydroxy oxane-2-carboxylic acid.

**Table 4**. Changes in the accumulation of 30 differential metabolities in *C. songaricum* across the developmental stages of tubercle (T), sprouting (S), unearthing (U), maturing (M), and atrophy (A) developmental stage using ultrahigh-performance liquid chromatography linked to quadruple time-of-flight mass spectrometry (UPLC-QTOF/MS) analysis. Ten samples as replicates were detected from each developmental stages.

| Name | mean±SD (n = 10) | | | | |
|---|---|---|---|---|---|
| | T | S | U | M | A |
| 4-Hydroxybenzaldehyde | 3052054±974079.8731 | 2349988±1030667.6990* | 1797975±197398.8644** | 3696610±1249226.9760 | 2435452±667730.8568* |
| Maltol | 5466980±1652325.4770* | 4527786±1225697.5600** | 4186563±1482629.4890** | 7522294±1847422.2300 | 6536740±2041205.6250 |
| Phenylglyoxal | 2601581±976131.4279 | 1767475±966177.5521* | 1236669±231346.4457** | 3101970±1347034.8430 | 1797859±563412.0762* |
| 3,4-Dihydroxybenzaldehyde | 6692251±2596449.7240 | 4722502±970534.4062** | 4378398±1536202.3430 | 6001045±702001.9179 | 4566337±1497013.7270* |
| HMBA[a] | 12863905±568736.0911 | 11323738±1048794.3430** | 10683573±2153598.3930** | 13486784±814527.5957 | 11887307±1412353.9930** |
| 2-Methylfuran | 1007852±273519.3367 | 624210±363458.6314 | 327635±323745.1858** | 825457±227496.2227 | 483610±385135.2597* |
| Dimethyl trisulfide | 1413753±258615.4354** | 565109±393592.7170* | 251477±353631.2520** | 906374±264866.1238 | 435924±493473.5895* |
| 4-*O*-Methylgallic acid | 2804158±587829.0458* | 1121797±702431.9986 | 601656±403542.9241** | 1932974±1036703.8420 | 1760195±822185.7088 |
| 5-Ethynyl-5'-(1-propynyl)-2,2'-bithiophene | 13246±19533.5351** | 1040725±495288.9971** | 959408±568151.3280** | 139507±93613.6715 | 552117±998634.1667 |
| N-Nitrosothiazolidine-4-carboxylic acid | 1579760 ±284081.7400* | 656162±476466.5605 | 433136±420160.5731* | 1053089±526760.7750 | 798034±583314.2580 |
| D-Galactose | 6146219±1174645.0280* | 2499141±1393913.2460 | 1339882±989245.7267** | 3804354±1485630.5010 | 4015983±1917618.7500 |
| Urolithin C | 7604174±912203.2035 | 5579686±2412457.6690 | 5144753±1871919.6180** | 8435160±1252837.9190 | 6341496±1973650.1590* |
| BR-Xanthone B | 1657700±424885.8361 | 1292482±268404.1249** | 1211424±313072.5221* | 1947122±193752.0798 | 1565516±396925.8936* |
| Norartocarpanone | 5557428±1495578.7160 | 5037735±1915316.9250 | 4160929±766908.5086** | 6049982±491056.4182 | 4737300±870009.3376** |
| DDDB[b] | 5299646±2190820.4470 | 6080370±4197954.0600 | 3215349±1418759.5270 | 4795477±1212686.5750* | 3005056±1707066.7080* |
| Rotenone | 4962503±5633469.2440* | 324448±433278.3500 | 617032±1056347.9170 | 356607±343758.0758 | 147850±89830.9953 |
| Lactulose | 11924149±10368709.2800** | 750143±1237427.9060 | 841598±1222273.3190 | 816273±1154202.9230 | 3485684±5532552.6200 |
| Cochliophilin A | 6923094±3187667.5540** | 630285±334613.5589 | 344904±237326.7796 | 604151±492691.2268 | 2736513±1823162.6500** |
| 1D-Myo-inositol 3,4-bisphosphate | 511671±253381.8769 | 219492±188778.4111 | 74368±81658.6911** | 351300±201820.2842 | 276995±289767.4383 |
| DPOT[c] | 2727458±1150154.5770** | 1204665±1108806.8010 | 929287±593494.2595 | 487029±347628.8046 | 4388194±2770220.7160** |

| | | | | | |
|---|---|---|---|---|---|
| Aflatoxin G | 1954715±771962.2736 | 1693389±693790.3924* | 1444325±599287.4413** | 2469857±455188.4078 | 2209888±776659.3779 |
| 3,4-Dihydroxyphenacyl caffeate | 3485423±1567456.9980 | 2669929±881377.0149** | 1803953±1001807.4300** | 4764661±1735324.2330 | 2301070±846909.2224** |
| DPCM[d] | 2709314±499141.3230** | 500205±491794.1851 | 103390±53474.3325** | 610276±521630.9730 | 1258862±848913.9333 |
| Proanthocyanidin A1 | 1880808±383413.1097** | 1470401±728491.4324** | 1284322±534560.0540** | 2815238±814048.5444 | 2748300±1844331.6690 |
| Epicatechin 5-*O*-*β*-D-glucopyranoside-3-benzoate | 1571741±409796.9876** | 1339043±549377.9153** | 1182321±330641.1952** | 2054982±163447.3481 | 1309227±455168.3916** |
| Kaempferol 7-(6''-galloylglucoside) | 762077±341965.0748** | 616818±311808.6769** | 181081±169684.7474** | 1144015±193842.6597 | 374829±361505.8518** |
| procyanidin C1 | 1417573±653170.6734** | 1144137±668716.5061** | 247527±262471.9150** | 2183828±425770.2849 | 664931±733058.3847** |
| 3-Oxo-valproic acid CoA | 767809±218778.5229* | 553999±326227.0478** | 123518±129285.5461** | 1038770±210957.2988 | 326033±360127.6363** |
| Compound 1 | 1824992±430660.4145** | 643676±430769.4798* | 436161±544593.6436** | 1241532±233449.9802 | 631797±517906.8134** |
| Compound 2 | 1086532±735713.7158** | 1800644±463492.3444** | 2526403±969412.1308** | 3966564±868224.3731 | 1494162±835465.2780 |

[a]HMBA: (±)-2-Hydroxy-4-(methylthio)butanoic acid.

[b]DDDB: 3-(3,4-dihydroxyphenyl)-3,4-Dihydro-2H-1-benzopyran-4,6,7-triol.

[c]DPOT: 6-{[3-(3,4-dihydroxyphenyl)propanoyl]oxy}-3,4,5-trihydroxyoxane-2-carboxylic acid.

[d]DPCM: 6-(2-{8,8-dimethyl-2-oxo-2H,8H-pyrano[2,3-f]chromen-3-yl}-5-methoxyphenoxy)-3,4,5-tri-hydroxyoxane-2-carboxylic acid.

*$P<0.05$ and **$P<0.01$ represent significant and extremely significant (*t*-test in 'T', 'S', 'U' and 'A' stages compared with 'M' stage) in curve graph of relative content of differential metabolites from different developmental stages. SD: standard deviation values.

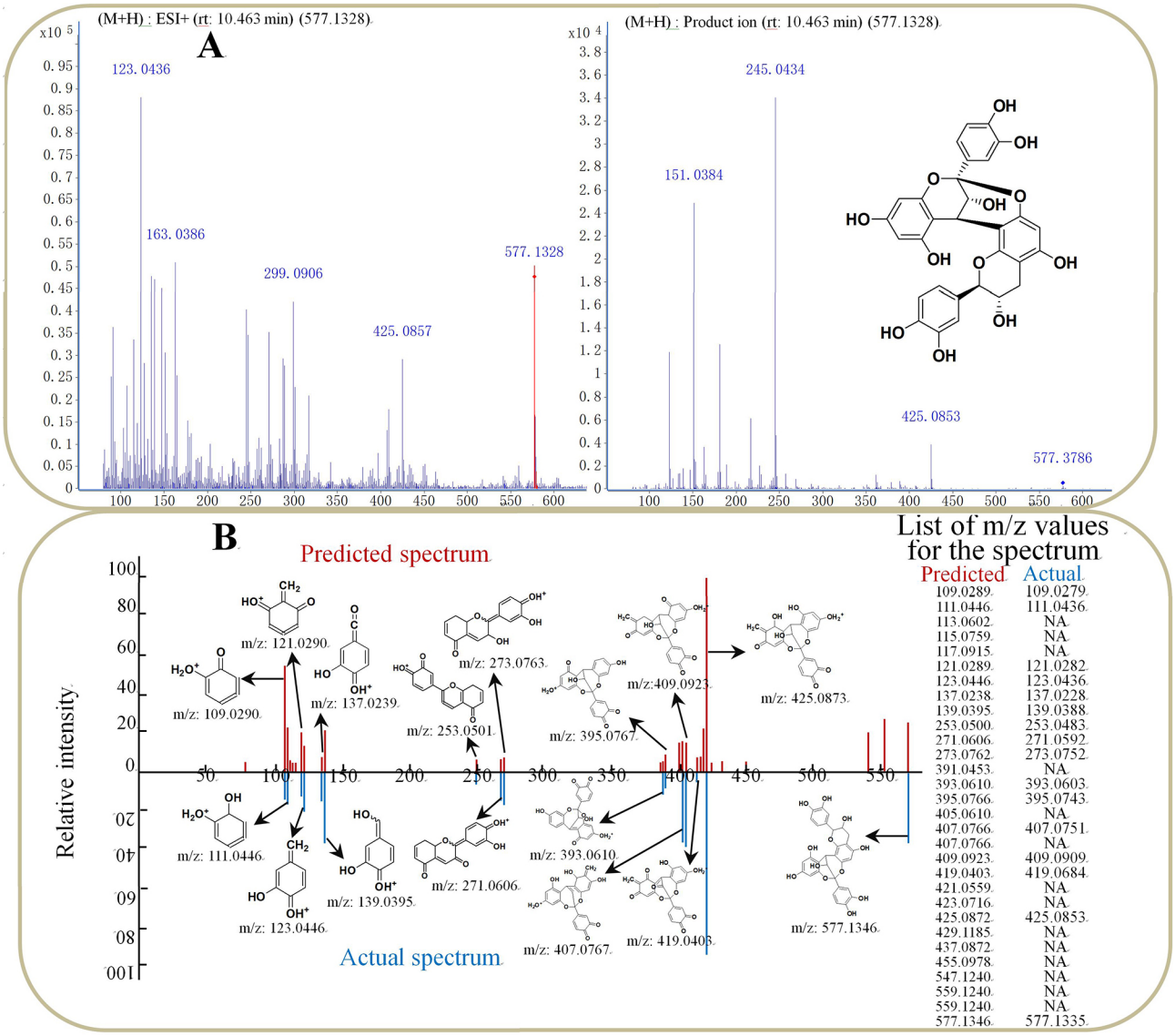


**Figure 2.** Mass spectrometric identification of the differential metabolite M577T8 as proanthocyanidin A1. Predicted MS/MS match with Agilent Mass Hunter Qualitative analysis in the PCDL database and the structure of the different metabolite (A). Predicted and actual list of m/z values for the differential metabolite spectrum and MS/MS match in the HMDB and METLIN databases (B).

The metabolic pathways are similar involved by differential metabolites between NMR and UPLC-QTOF/MS platforms. In different development stages, there were differences in the primary metabolism of *C. songaricum*, such as sugar metabolism and amino acid (protein) metabolism. In the secondary metabolism, flavonoids were main involvement. But in detail, the differential metabolites involved in sugar metabolism mainly include sucrose, maltose and malate in NMR analysis; but were D-galactose, lactulose and maltol in UPLC-QTOF/MS results. Cysteine, tyrosine, glutamate, alanine were involved in the amino acid metabolism based on NMR analysis while they were 4-hydroxybenzaldehyde,

3,4-dihydroxybenzaldehyde and 3,4-dihydroxyphenacyl caffeate in UPLC-QTOF/MS analysis.

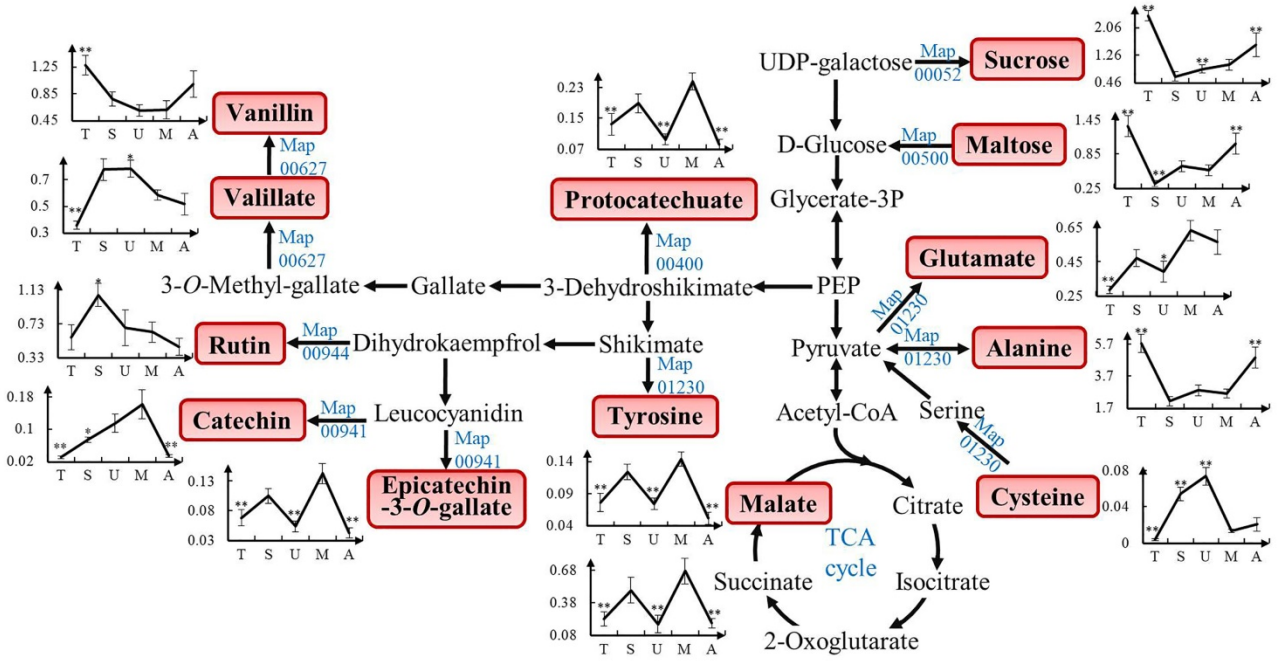


**Figure 3.** Metabolic pathway map of differential marker metabolites in *Cynomorium songaricum* from different developmental stages based on NMR. The pathways were verified by KEGG database, and the blue words are number of metabolic pathways of differential metabolites. $^{*}P<0.05$ and $^{**}P<0.01$ represent significant and extremely significant (*t*-test in 'T', 'S', 'U' and 'A' stages compared with 'M' stage) in curve graph of relative content of differential metabolites from different developmental stages.

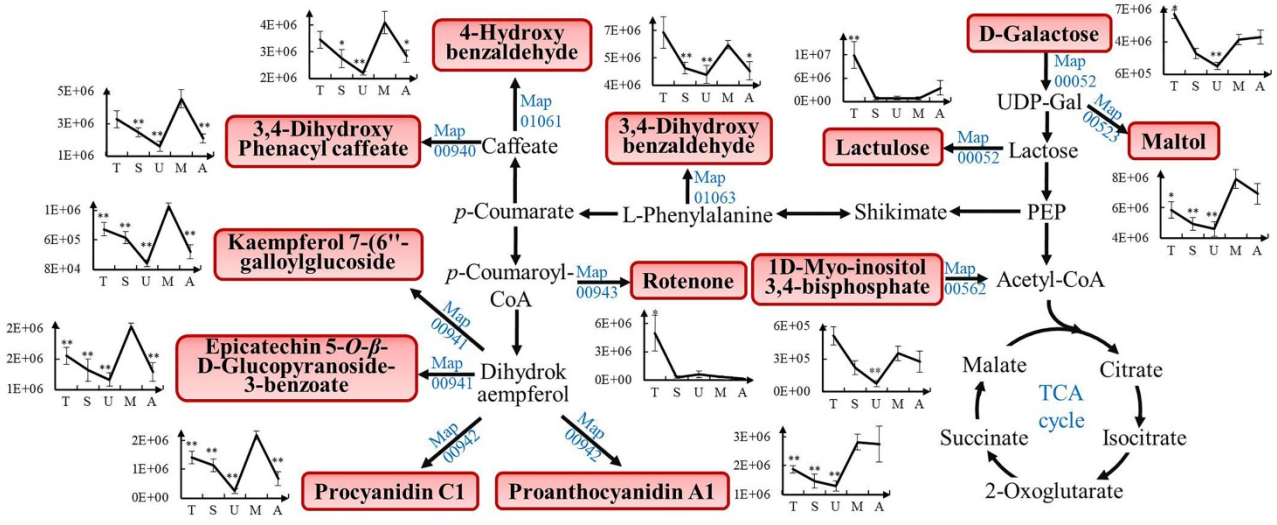


**Figure 4.** Metabolic pathway map of differential marker metabolites in *Cynomorium songaricum* from different developmental stages based on UPLC-QTOF/MS. The pathways were verified by KEGG database, and the blue words are number of metabolic pathways of differential metabolites. $^{*}P<0.05$ and $^{**}P<0.01$ represent significant and extremely significant (*t*-test in 'T', 'S', 'U' and 'A' stages compared with 'M' stage) in curve graph of relative content of differential metabolites from different developmental stages.

The biosynthesis pathways involved in flavonoids in NMR metabolomics analysis were catechin, epicatechin-3-*O*-gallate and rutin but were BR-xanthan B, proanthocyanidin A1, proanthocyanidin C1, kaempferol 7-(6''-galloylglucoside), epicatechin 5-*O*-*β*-D-glucopyranoside-3-benzoate and rotenone in UPLC-QTOF/MS. NMR analysis showed that protocatechuate was involved in the biosynthesis of antibiotics while maltol and an aflatoxin G may play a role with the UPLC-QTOF/MS analysis. There are other metabolic differences, for example, the NMR analysis showes that vanillin and vanillate were involved in the pathway of aminobenzoate degradation, and the UPLC-QTOF/MS analysis shows that 1D-myo-inositol 3,4-bisphosphate was involved in inositol phosphate metabolism.

## 4. DISCUSSION

Due to the diversity of metabolites in chemistry structure and type, multi-technological platforms are utilized to study the difference of plant metabolism, which greatly improves the quality evaluation of plant. Dastmalchi *et al*. (2014) demonstrated the advantages of simultaneous use of NMR and UPLC-QTOF/MS to analyze different aspects of the plant metabolome in the same study. NMR technology has merits of excellent reproducibility, fast speed, uncomplicated sample preparation and strong quantitative ability for compounds, but its low sensitivity impedes the detection of low concentration metabolites in samples (WISHART, 2011). In contrast, UPLC-QTOF/MS has higher sensitivity and molecular specificity but lack of lots of standard compounds and comprehensive MS/MS database hinders rapid and reliable identification of a large number of metabolites (Want *et al*., 2010). However, the unique physicochemical principles of NMR and UPLC-QTOF/MS make these two technologies complementary to each other. Both techniques used in one study can achieve the most comprehensive profiling of the entire metabolome (Beltran *et al*., 2012). In this study, the primary metabolites of *C. songaricum*, such as sugar and amino acid (protein) were mainly detected by NMR while the secondary metabolites mainly detected based on UPLC-QTOF/MS. Thus combined use of two or more platforms together to study metabolomics is still significant for systematic and objective metabolomics study.

Although the detected chemicals were not are not exactly the same, the chemical types were consistent between NMR and UPLC-QTOF/MS in this study. They include flavonoids, organic acids, sugars, amino acids and other substances, which are involved in the same metabolic pathways. Differential metabolites from NMR contain more primary metabolites, sugars and amino acids are the highest in 'T' stage, for energy storage of the development of *C. songaricum.* In 'S' and other development stages, the energy was used for germination and growth, then primary metabolites are transformed into secondary metabolites or secondary metabolites transformed each other for specific purpose. For example, the relative contents of the vanillate and vanillin are negatively correlated across all stages (Figure 3), and they might be transformed each other in metabolic process. UPLC-QTOF/MS detected a large proportion of differential secondary metabolites, and their types and contents reach higher level in 'U' and 'M' stages, indicating that the effective components in 'U' and M' stages were much higher than those in other stages, and the bioactive quality of *C. songaricum* was better (MENG *et al*., 2013). Thus this study can provide help in assessing the pharmacological effects of *C. songaricum* collected from different seasons.

The difference of metabolic composition of *C. songaricum* was also influenced by many other factors. Our group have used UPLC-QTOF/MS platform to study the correlation between metabolites and endophytic fungi of *C. songaricum* in the 'U' stage from different locations, and found that metabolites were not only related to environmental factors and gene regulation, but also related to internal environmental biological factors (CUI *et al*., 2018c; CUI *et al*., 2019). In both studies, the differential metabolites and the metabolic pathways involved were similar. However, though the *C. songaricum* samples collected in different years, different locations, even if the collection season and instrument platform are the same, the metabolites are still quite different. Therefore, there is still a long way to go to clearly study the metabolic differences between plants (DELFIN *et al*., 2019).
In summary, for the first time, this study obtained the data of metabolic difference of *C. songaricum* in different developmental stages based on UPLC-QTOF/MS and NMR, which will provide help to understand metabolite accumulations of *C. songaricum*, and will also assist people to establish new ideas and methods for the evaluation of *C. songaricum*.

## ACKNOWLEDGEMENTS

The authors thank the Scientific Instrument Center of Shanxi University of China for technical support.
This work was supported by the National Natural Science Foundation of China (No. 31670328, 31270383).

## REFERENCES

Beltran A., Suarez M., Rodríguez M.A., Vinaixa M., Samino S., Arola L., Correig X. and Yanes O. 2012. Assessment of compatibility between extraction methods for NMR and LC/MS-based metabolomics. Anal. Chem. 84(14):5838-44.

Chang Y.X., Li J., Su G.R. and Wang Y.C. 2007. Study on the dynamics trends of polysaccharide content of *Cynomorium songaricum* Rupr. in different growth stages. J. Inner Mongolia U. 2:237-240.

Chen J., Leong P.K., Leung H.Y., Chan W.M., Wong H.S. and Ko K.M. 2019. 48 Biochemical mechanisms of the anti-obesity effect of a triterpenoid-enriched extract of *Cynomorium songaricum* in mice with high-fat-diet-induced obesity. Phytomedicine. 153038.

Committee for the Pharmacopoeia of PR China. (Ed.). 2015 "Pharmacopoeia of PR China". Chinese Medical Science and Technology Press, Beijing, China.

Cui J.L., Vijayakumar V. and Zhang G. 2018b. Partitioning of fungal endophyte assemblages in root-parasitic plant *Cynomorium songaricum* and its host *Nitraria tangutorum*. Front Microbiol. 9:666.

Cui J.L., Gong Y., Vijayakumar V., Zhang G., Wang M.L., Wang J.H. and Xue X.Z. 2019. Correlation in chemical metabolome and endophytic mycobiome in *C. songaricum songaricum* from different desert locations in China. J. Agric. Food Chem. 67(13):3554-3564.

Cui J.L., Gong Y., Xue X.Z., Zhang Y.Y., Wang M.L. and Wang J.H. 2018a. A phytochemical and pharmacological review on *C. songaricum* as functional and medicinal food. Nat. Prod. Commun. 13:501.

Cui J.L., Zhang Y.Y., Vijayakumar V., Zhang G., Wang M.L. and Wang J.H. 2018c. Secondary metabolite accumulation associates with ecological succession of endophytic fungi in *C. songaricum songaricum* Rupr. J. Agric. Food Chem. 66:5499.

Cui Z., Guo Z., Miao J., Wang Z., Li Q., Chai X. and Li M. 2013. The genus *Cynomorium* in China: an ethnopharmacological and phytochemical review. J. Ethnopharmacol. 147(1):1-15.

Dastmalchi K., Cai Q., Zhou K., Huang W., Serra O. and Stark R.E. 2014. Solving the jigsaw puzzle of wound-healing potato cultivars: metabolite profiling and antioxidant activity of polar extracts. J. Agric. Food Chem. 62:7963-75.

Delfin J.C., Watanabe M. and Tohge T. 2019. Understanding the function and regulation of plant secondary metabolism through metabolomics approaches. Theor. Exp. Plant Physiol. 31:127-138.

Deshmukh R., Sharma L., Tekade M., Kesharwani P., Trivedi P. and Tekade R.K. 2016. Force degradation behavior of glucocorticoid deflazacort by UPLC: isolation, identification and characterization of degradant by FTIR, NMR and mass analysis. J. Biomed. Res. 30:149-161.

Ghatak A., Chaturvedi P. and Weckwerth W. 2018. Metabolomics in Plant Stress Physiology. Adv. Biochem. Eng. Biotechnol. 164:187-236.

Huang X.W. 1997. Preliminary studies on tannins of *Cynomorium songaricum* Rupr. J. Inner Mongolia Trad. Chin. Med. S1:119-120.

Jiang Z.H., Tanaka T., Sakamoto M., Jiang T. and Kouno I. 2001. Studies on a medicinal parasitic plant: lignans from the stems of *Cynomorium songaricum.* Chem. Pharm. Bull. 49: 1036-1038.

Jin S.W., Eerdunbayaer A.D., Kuroda T., Zhang G.X., Hatano T. and Chen G.L. 2012. Polyphenolic constituents of *Cynomorium songaricum* Rupr. and antibacterial effect of polymeric proanthocyanidin on methicillin-resistant staphylococcus aureus. J. Agric. Food Chem. 60:7297-7305.

Johnson C.H., Ivanisevic J. and Siuzdak G. 2016. Metabolomics: beyond biomarkers and towards mechanisms. Nat. Rev. Mol. Cell Biol. 17:451.

Liu Y., Li H., Wang X., Zhang G., Wang Y. and Di D. 2011. Evaluation of the free radical scavenging activity of *Cynomorium songaricum* Rupr. by a novel DPPH-HPLC method. J. Food Sci. 76(9):C1245-9.

Ma C.M., Jia S.S., Sun T. and Zhang Y.W. 1993. Triterpenes and steroidal compounds from *Cynomorium songaricum.* Acta. Pharm. 28:152-155.

Ma C.M., Nakamura N., Hattori M. and Cai S.Q. 2002. Isolation of malonyl oleanolic acid hemiester as anti-HIV protease substance from the stems of *Cynomorium songaricum.* Chin. Pharm. J. 37:336-338.

Ma C.M., Nakamura N., Miyashiro H., Hattori M. and Shimotohno K. 1999. Inhibitory effects of constituents from *Cynomorium songaricum* and related triterpene derivatives on HIV-1 protease. Chem. Pharm. Bull. 47:141-145.

Meng H.C. and Ma C.M. 2013. Flavan-3-ol-cysteine and acetylcysteine conjugates from edible reagents and the stems of *Cynomorium songaricum* as potent antioxidants. Food Chem. 141:2691-2696.

Meng H.C., Wang S., Li Y., Kuang Y.Y. and Ma C.M. 2013. Chemical constituents and pharmacologic actions of *C. songaricum* plants. Chin. J. Nat. Med. 11(4):321-9.

Muhammad A., Tel-Çayan G., Öztürk M., Duru M.E., Nadeem S., Anis I., Ng S.W. and Shah M.R. 2016. Phytochemicals from *Dodonaea viscosa* and their antioxidant and anticholinesterase activities with structure-activity relationships. Pharm. 54:1649-55.

Raju C.K., Pandey, A.K., S G., Ghosh K., Pola A., Goud P.S.K., Jaywant M.A. and Navalgund S.G. 2017. Isolation and characterization of novel degradation products of Doxofylline using HPLC, FTIR, LCMS and NMR. J. Pharm. Biomed. Anal. 140:1-10.

Wang X.M., Zhang Q., Rena K., Wang X.L. and Wang X.Q. 2011. Chemical constituents in whole plant of *Cynomorium songaricum.* Chin. Trad. Herbal Drugs. 42:458-460.

Want E.J., Wilson I.D., Gika H., Theodoridis G., Plumb R.S., Shockcor J., Holmes E. and Nicholson J.K. 2010. Global metabolic profiling procedures for urine using UPLC-MS. Nat. Protoc. 5(6):1005-18.

Wishart D.S. 2011. Advances in metabolite identification. Bioanal. 3(15):1769-82.

Xu X., Zhang C. and Li C. 1996. Chemical components of *Cynomorium songaricum* Rupr. China Chin. Mater. Med. 21:676-677.

Zampieri M., Sekar K., Zamboni N. and Sauer U. 2017. Frontiers of high-throughput metabolomics. Curr. Opin. Chem. Biol. 36:15-23.

Zhang B.S., Lu X.S., Zhang R.Z. and Gu L.Z. 1990. Research on relaxing the bowels components of *Cynomorium songaricum* Rupr. J. Chin. Med. Mat. 13:36-38.

Zhang C.Z., Xu X.Z. and Li C. 1996. Fructosides from *Cynomorium songaricum.* Phytochem. 41:975-976.

Zhang L., Pei D., Huang Y.R., Wei J.T., Di D.L. and Wang L.X. 2016. Chemical constituents from *Cynomorium songaricum*. J. Chin. Med. Mat. 39:74-77.

Zhang Q. 2007. Fundamental studies of chemical constituents of *Cynomorium songartcum* Rupr. Xinjiang Med. U. 6-9.

Zhang Q., Rena K. and Wang X.M. 2007b. Studies on the chemical constituents of flavonids in the inflorescences of *Cynomorium songaricum* Rupr. J. Xinjiang Med. U. 30:466-468.

Zhang S.J., Wang Y.W., Liu L., Yu J.Y. and Hu J.P. 2007a. Study on chemical constituents of herba *Cynomorii.* Chin. Pharm. J. 42:975977.

Zhi H.J., Qin X.M., Sun H.F., Zhang L.Z., GuoX.Q. and Li Z.Yu. 2012. Metabolic fingerprinting of *Tussilago farfara* L. using $^{1}$H-NMR spectroscopy and multivariate data analysis. Phytochem. Anal. 23:492-501.

Paper Received May 20, 2020 Accepted July 16, 2020